Journal of Power Sources, 41 (1993) 291–298

Single- and double-ion type cross-linked polysiloxane solid electrolytes for lithium cells

Hiromori Tsutsumi, Masahiro Yamamoto, Masayuki Morita and Yoshiharu Matsuda
Department of Applied Chemistry and Chemical Engineering, Faculty of Engineering, Yamaguchi University, Ube 755 (Japan)

Takashi Nakamura and Hiroyuki Asai
Dow Corning Toray Silicone Co., Ltd., 2-2 Tigusa-kaigan, Ichihara 299-02 (Japan)

(Received July 10, 1992; in revised form September 25, 1992)

Abstract

Polymeric solid electrolytes, that have poly(dimethylsiloxane) (PMS) backbone and cross-linked network, were applied to a rechargeable lithium battery system. Single- (PMS–Li) and double-ion type (PMS–$LiClO_4$) electrolytes were prepared from the same prepolymers. Lithium electrode in the both electrolytes showed reversible stripping and deposition of lithium. Intercalation and deintercalation processes of lithium ion between lithium–manganese composite oxide (Li_xMnO_2) electrode and the electrolytes were also confirmed by cyclic voltammetry, however, peak current decreased with several cycles in both cases. The model cell, Li/PMS–Li/Li_xMnO_2 cell had 1.4 mA h g^{-1} (per 1 g of active material, current density: 3.77 μA cm^{-2}), and the Li/PMS–$LiClO_4$/Li_xMnO_2 cell had 1.6 mA h g^{-1} (current density: 75.3 μA cm^{-2}).

Introduction

Development of lithium batteries for high energy storage has continued since 1970. Commercially-available Li batteries usually have organic liquid electrolyte [1]. When the cell has a liquid electrolyte, the cell is heavy and its container must be perfectly sealed to protect against electrolyte leakage. Application of polymeric solid electrolytes to a Li battery system will produce a lightweight cell with high energy density [2–4]. However, polymeric solid electrolytes have some problems for practical use. Their conductivity is lower than that of liquid electrolytes, and they are slightly unstable.

We selected a polysiloxane polymer for matrix of polymeric solid electrolytes in a Li battery system. Polysiloxane polymers have good properties for the matrices, low glass-transition temperature because of their flexible backbone, and chemical and mechanical stability [5]. Some polysiloxane solid electrolytes were studied and their advantages were reported [6–8]. Previously, we reported on the preparation method of novel polymeric solid electrolytes with polysiloxane backbone and their basic properties [9]. The solid electrolytes had several preferable properties such as high ionic conductivity and stability. The most characteristic point of the electrolytes is that single- and double-ion type polymeric solid electrolytes can be prepared from same prepolymers by changing the dissolved Li salts. In this work we apply the two different types of polysiloxane solid electrolytes to a Li battery system. Electrochemical behavior of Li and positive

0378-7753/93/$6.00

active material-electrode in the polymeric solid electrolytes, and charge/discharge properties of model cells are reported.

Experimental

Materials

$LiClO_4$ and LiOH were purchased from Ishizu Seiyaku and dried at 120 °C for 24 h before use. A Li electrode was prepared by pressing a Li foil (thickness 0.2 mm, Mitsui Mining & Smelting) on a nickel gauze.

Polysiloxane solid electrolytes

The preparation method of the polysiloxane solid electrolytes was reported in detail in ref. 9. Figure 1 shows the molecular structure of the polymers.

The polymer was prepared by cross-linking reaction between two types of oligosiloxanes, one has some carbonyl groups and another has some hydroxyl groups in the side chains. Poly(dimethylsiloxane) (PMS)–Li is a single-, and PMS–$LiClO_4$ that contains $LiClO_4$ is a double-ion type polymeric solid electrolyte. Typical size of the film was 13 mm in diameter and 0.3–0.5 mm thick.

Lithium–manganese composite oxide (Li_xMnO_2) electrode

Lithium–manganese composite oxide was prepared according to the method reported by Nohma *et al.* [10, 11]. A mixture (molar ratio of Li:Mn = 3:7) of LiOH and MnO_2 (I.C. no. 12) was heated at 375 °C for 20 h in air. The product is a composite oxide of γ/β-MnO_2 and Li_2MnO_3 [10, 11].

Disk-shaped tablet electrodes of Li_xMnO_2 were prepared from a mixture of 30 mg of Li_xMnO_2, 20 mg of acetylene black and 5 mg of Teflon powder, by pressing. At this time, a nickel gauze as a current collector was also attached on the side of the disk. The tablet has a diameter of 13 mm and an average thickness of 0.5 mm. When the mixing ratio of Teflon powder was low, the tablet was brittle.

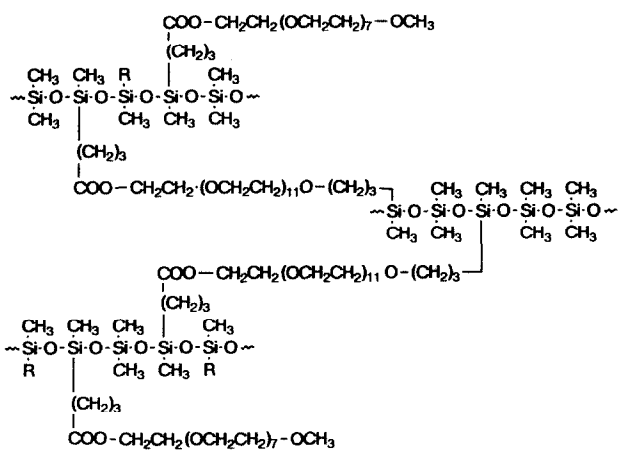

Fig. 1. Schematic representation of PMS–Li and PMS–$LiClO_4$.

Measurements

All cell construction and electrochemical measurements were performed in a dry box under argon gas at room temperature (20–25 °C). The cell for polarization curve measurements has a square Li electrode (surface 4 mm×4 mm) as working, a circular Li electrode (diameter: 13 mm) as counter, and a Li slip (surface: 1 mm×2 mm) as a reference electrode. Figure 2 shows their configuration.

Polarization curves were measured with a potentiogalvanostat (Nikko Keisoku, NPGS-5) and the quasi steady-state current was recorded in 0.1 V steps from 0 V versus Li/Li^+ to ±1.5 V and backward, potentiostatically at room temperature (20–25 °C). Micropolarization curves (at 25 °C) were measured by using the same cell, and the current was recorded after 2 min at a quasi steady state. The IR drops in the electrode potentials were measured by the current pulse measurement, and the potential was corrected [12].

Cyclic voltammetry

A polymeric solid electrolyte film was sandwiched between the modified MnO_2 electrode (a quarter size of the pressed tablet: 0.33 cm^2) as a working electrode and Li electrode (diameter: 13 mm) as a counter electrode. Reference electrode (Li slip; surface: 1 mm×2 mm) was set near the working electrode (the gap was 1 mm). The measurements were performed with a potentiogalvanostat (Nikko Keisoku, NPGS-5), function generator (Nikko Keisoku, NFG-5), and *x–y* recorder (Graphtec, WX-1100) at room temperature (20–25 °C). Scan rate was 1 mV s^{-1}.

Charge/discharge cycling of model cell

The test cell had a lithium–manganese composite oxide electrode, a Li electrode, and a polymeric solid electrolyte (PMS–Li or PMS–$LiClO_4$) film. The film was sandwiched between the electrodes. The size of those electrodes and the film was 13 mm in diameter and typical total thickness was 1.0–1.2 mm. The model cell was constructed in a dry box under argon atmosphere.

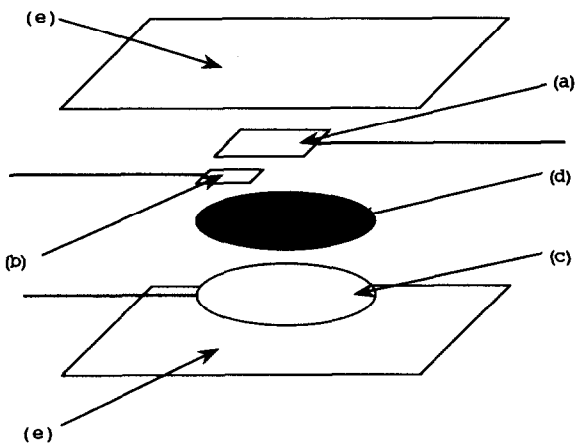

Fig. 2. Schematic representation of the cell for polarization measurements: (a) working electrode (Li foil, surface: 4 mm×4 mm); (b) reference electrode (Li foil, surface: 1 mm×2 mm); (c) counter electrode (Li foil, diameter: 13 mm); (d) polymeric solid electrolyte, and (e) Teflon plate.

Charge/discharge experiments of the cell were carried out on a charge/discharge controller (PMS–$LiClO_4$, Nikko Keisoku NCD-1S and PMS–Li, handmade controller) with preset cutoff voltage at 3.5 and 2.5 V with constant current (PMS–$LiClO_4$: 75.3 $\mu A\ cm^{-2}$ and PMS–Li: 3.77 $\mu A\ cm^{-2}$, respectively) at room temperature (20–25 °C).

Results and discussion

Properties of network polysiloxane electrolytes

Figure 1 shows the structure of polysiloxane electrolytes. Both single- and double-ion type electrolytes have PMS backbones and network cross-linked by ester bonds. Their side chains are oligoethylene oxide chains for solvation of Li ions. In the case of the single-ion type electrolyte, counter anions are $-COO^-$ groups in the polymer chains. Transference number of Li^+ was 0.98, because the anionic units are immobile [9]. The conductivity of the film at 25 °C was 1.0×10^{-6} S cm^{-1}.

We also prepared double-ion type polymeric solid electrolytes with various Li salts, such as $LiClO_4$, $LiBF_4$, $LiPF_6$, $LiAsF_6$, and $LiCF_3SO_3$. The polymeric solid electrolyte that contains $LiClO_4$ salt (PMS–$LiClO_4$) was chemically stable and had higher conductivity (3.2×10^{-5} S cm^{-1}, at 25 °C) than those containing other salts.

Thermal properties of the electrolyte films were tested by TG/DTA measurements (heating rate 10 K min^{-1}). Both electrolytes were thermally stable. When they were heated from room temperature to 220 °C in air, no obvious decrease in their mass was observed. These films were thermally stable in air.

Polarization behavior of lithium electrode in the polymeric solid electrolytes

On application of a polymeric solid electrolyte to a secondary Li battery, the reversibility of Li electrode reaction in an electrolyte is one of the essential properties. The reversibility of Li electrode in PMS–Li and PMS–$LiClO_4$ was checked by polarization measurements at room temperature.

Using the cell as shown in Fig. 2, the polarization behavior of Li electrodes in PMS–Li and PMS–$LiClO_4$ was investigated. Figure 3 shows the quasi steady-state polarization curves of Li in PMS–$LiClO_4$ and PMS–Li. The measurements were started

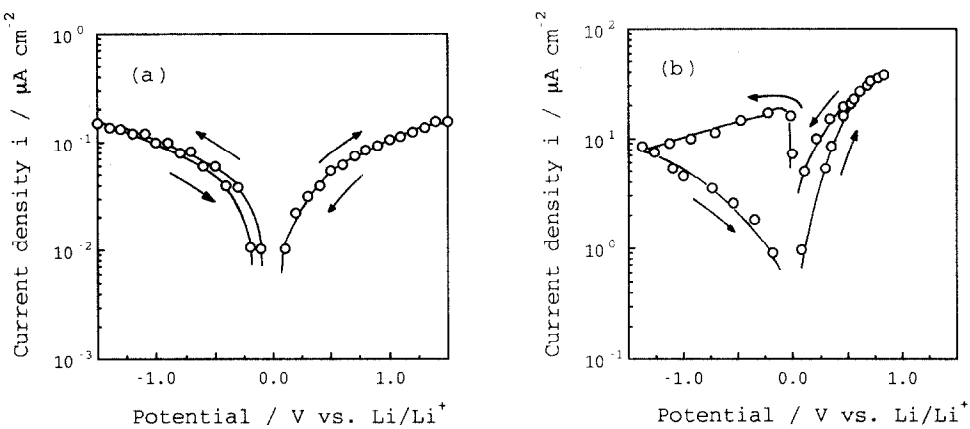

Fig. 3. Polarization curves of lithium in (a) PMS–Li and (b) PMS–$LiClO_4$ at room temperature, ~20–25 °C.

at 0 V versus Li/Li^+ and the current was recorded potentiostatically. IR loss in the resulting curves was corrected by the current pulse measurements [12].

Figure 3(a) shows the curves for PMS–Li electrolytes. Both branches, anodic and cathodic, are symmetrical. This indicates that both the stripping and plating processes of Li between the Li electrode and the electrolyte film are reversible. This property is required for its application in rechargeable Li batteries.

Figure 3(b) shows the curves for the PMS–$LiClO_4$ film. In the anodic polarization, both curves that were measured with a polarization from 0 to 1.5 V, and from 1.5 to 0 V, agree with each other. In the cathodic polarization, a hysteresis was observed. This phenomenon was also observed in other double-ion type polymeric solid electrolyte system [12]. This hysteresis is probably caused by decreasing in Li^+ concentration at the Li electrode. The rate of Li^+ diffusion in the bulk of PMS–$LiClO_4$ is lower than that of charge transfer at the electrode interface. Thus, the deficiency of the Li^+ cannot be sufficiently compensated by diffusion of Li^+. In the anodic case, stripping of Li to the electrolyte kept the concentration of Li^+ constant. Thus, such hysteresis did not appear.

Exchange current density for lithium electrode reaction in PMS–Li and PMS–$LiClO_4$

When a solid electrolyte is used in a high current density Li battery, the value of exchange current density for Li electrode reaction in the electrolyte becomes a key point. Using the micropolarization technique of Li in PMS–Li and PMS–$LiClO_4$, the values of exchange current density (i_0) for Li electrode in the electrolytes were estimated [12]. The value of polarization resistance, θ, was from the slope of micropolarization measurements under a steady-state galvanostatic condition at 25 °C:

$$i_0 = RT/2F\theta \tag{1}$$

The exchange current density was 11 $\mu A\ cm^{-2}$ in PMS–$LiClO_4$ and 0.54 $\mu A\ cm^{-2}$ in PMS–Li, respectively. These values are rather small compared with those for poly(ethylene oxide) (PEO)-based solid electrolyte (450 $\mu A\ cm^{-2}$) [13] and PEO-grafted polymer with $LiClO_4$ salt (84 $\mu A\ cm^{-1}$) [12]. It indicates that the rate of charge transfer in PMS–Li and PMS–$LiClO_4$ is lower than that in PEO-based electrolytes. An increase in the exchange current density for PMS–Li and PMS–$LiClO_4$ systems need to ensure their practical application.

Electrochemical behavior of lithium–manganese composite oxide (Li_xMnO_2) electrode in PMS–Li and PMS–$LiClO_4$ electrolytes

Many Li intercalation compounds, such as those with MnO_2, V_6O_{13}, TiS_2 and Fe_2O_3 have been considered, and used as possible positive electrodes for Li batteries [10, 11, 14–17]. To test the cycleability of the Li intercalation/deintercalation processes in such compounds, we selected lithium–manganese composite oxide (Li_xMnO_2) which is a composite of γ/β-MnO_2 and Li_2MnO_3 [10, 11], because of their very simple preparation method. Electrochemical behavior of the Li_xMnO_2 electrode in PMS–Li or PMS–$LiClO_4$ was investigated by cyclic voltammetry. The electrode potential was recorded against at the Li/Li^+ electrode. Scan rate was 1 $mV\ s^{-1}$.

Figure 4(a) is cyclic voltammogram that shows the cycleability of the Li_xMnO_2 electrode in PMS–Li. Peaks at 3.2 V on anodic scan, and at 2.5 V on cathodic scan, were observed. Both peaks correspond to deintercalation and intercalation of Li ions for Li_xMnO_2 [10, 11]. Figure 4(b) shows the cycleability of the Li_xMnO_2 electrode in PMS–$LiClO_4$. On the anodic scan, a peak that corresponds to deintercalation of Li was observed at 3.8 V versus Li/Li^+. During the cathodic scan, a peak at 2.5 V that

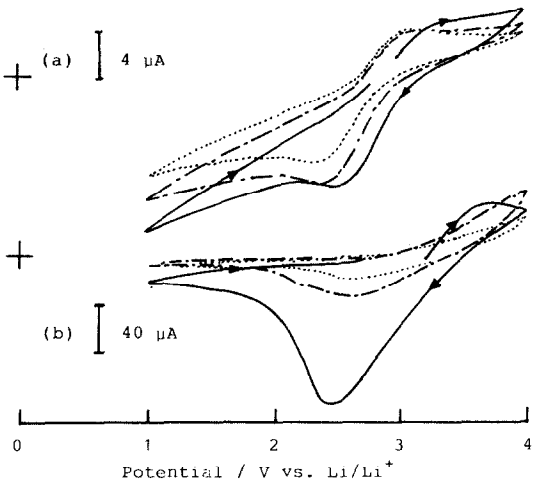

Fig. 4. Cyclic voltammograms for Li_xMnO_2 electrode in (a) PMS–Li and (b) PMS–$LiClO_4$ electrolyte at room temperature. Scan rate is 1 mV s^{-1}. (——): 1st scan, (– – –): 5th scan, (- - - -): 10th scan.

corresponds to intercalation of Li^+ in the polymeric solid electrolyte was also observed. The peak current decreased after repeated scanning in both PMS–Li and PMS–$LiClO_4$ systems. Some irreversible reactions in the electrode or interphase of electrode (e.g. a crystal lattice degradation of Li_xMnO_2 or a loss of ionic and/or electronic contact between the electrode and the electrolyte [18]) may occur under cyclic voltammetry condition.

Cycling test of model cells

Using PEO-based electrolytes, for example, $(PEO)_8$–$LiClO_4$/10 wt.% β-Al_2O_3 [19], $(PEO)_{12}$–$LiClO_4$ [20], all solid-state secondary Li batteries were constructed and demonstrated their cycling performance. We also tested some model cells with the two types of polymeric solid electrolytes. The test cells consisted of Li foil, Li_xMnO_2 electrode, and PMS–Li or PMS–$LiClO_4$ film. The polymeric solid electrolyte film was sandwiched between the Li and Li_xMnO_2 electrodes (diameter: 13 mm). The open-circuit voltage of the cells was in the range 2.7–2.8 V at room temperature (20–25 °C).

Figure 5 shows charge/discharge curves of the cells. Cycling of the cells under constant-current conditions was performed between 2.5 and 3.5 V as cutoff voltage. Figure 5(a) shows the charge/discharge curves in the cell using PMS–Li electrolyte at a constant current of 3.77 μA cm^{-2} during the 1st, 12th and 17th cycles. Figure 6(a) shows changes in the discharge capacity of the cell with cycle number. Capacity of Li/PMS–Li/Li_xMnO_2 was 1.36 mA h g^{-1} (per 1 g of active material) under these conditions. Figure 5(b) shows the charge/discharge curves in the cell using PMS–$LiClO_4$ at a constant current of 75.3 μA cm^{-2} during the 1st, 10th, and 16th cycles. Discharge performance is shown in Fig. 6(b). The cell capacity was 1.6 mA h g^{-1}. Both cells did not utilize the theoretical capacity (above 250 mA h g^{-1} [10, 11]) of Li_xMnO_2. In this experimental condition, the amount of Li was enough for the cycling test. Thus, the capacity deficiency of these cells may be caused by an incomplete Li ion diffusion from the electrolytes to all active sites of positive active material. The

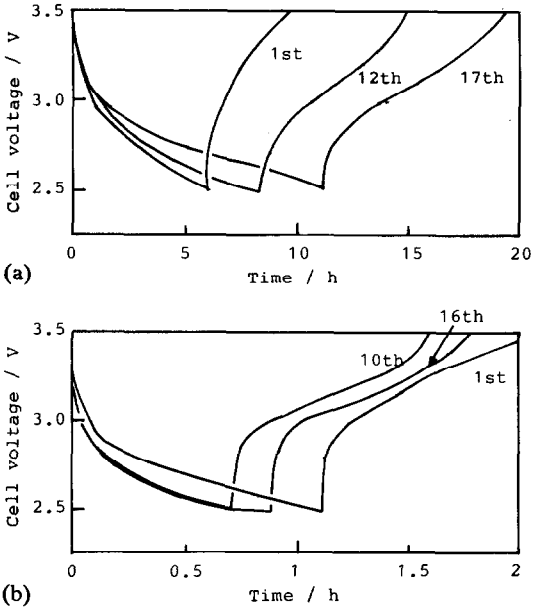

Fig. 5. Charge/discharge curves for model cell at room temperature: (a) Li/PMS–Li/Li_xMnO_2, charge and discharge current: 3.77 μA cm^{-2}, and (b) Li/PMS–$LiClO_4$/Li_xMnO_2, charge and discharge current: 75.3 μA cm^{-2}.

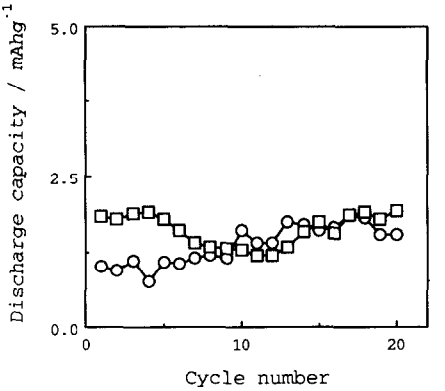

Fig. 6. Cycle number–discharge capacity for the model cell, charge/discharge condition is presented in Fig. 5. (○): Li/PMS–Li/Li_xMnO_2, and (□): Li/PMS–$LiClO_4$/Li_xMnO_2.

composition and structure of the positive electrode should be optimized for increasing in the cell capacity and cycling performance.

Acknowledgement

This work was supported in part by the Electric Technology Research Foundation of Chugoku.

References

1 Y. Matsuda and C. R. Schlaikjer (eds.), *Practical Lithium Batteries,* JEC Press, Cleveland, OH, 1988.
2 J. S. Tonge and D. F. Shriver, in J. H. Lai, (ed.), *Polymer Electrolytes in Polymers for Electronic Applications,* CRC Press, Boca Raton, FL, 1989, pp. 157–210.
3 B. Scrosati, in J. R. Akridge and M. Balkanski (eds.), *Chemistry, Physics and Applications of Polymeric Solid Electrolytes to Microbatteries in Solid State Microbatteries,* Plenum, New York, 1990, pp. 103–143.
4 M. Armand, *Adv. Mater. Res., 2* (1990) 278.
5 E. G. Rochow (ed.), *Silicon and Silicones,* Springer, Berlin, 1987.
6 Z. Ogumi, Y. Uchimoto and Z. Takehara, *J. Power Sources, 26* (1989) 457.
7 H. L. Mei, Y. Okamoto, T. Skotheim and C. S. Harris, *Mol. Cryst. Liq. Cryst., 160* (1990) 321.
8 Chang-Jyh Hsieh, Ging-Ho Hsiue and Chan-Shu Hsu, *Makromol. Chem., 191* (1990) 2195.
9 H. Tsutsumi, M. Yamamoto, M. Morita, Y. Matsuda, T. Nakamura and H. Asai, *Electrochim. Acta, 37* (1992) 1183.
10 T. Nohma, T. Saito, N. Furukawa and H. Ikeda, *J. Power Sources, 26* (1989) 389.
11 T. Nohma, Y. Yamamoto, K. Nishio, I. Nakane and N. Furukawa, *J. Power Sources, 32* (1990) 373.
12 M. Morita, T. Fukumasa, M. Motoda, H. Tsutsumi, Y. Matsuda, T. Takahashi and H. Ashitaka, *J. Electrochem. Soc., 137* (1990) 3401.
13 S. Morzilli, F. Bonino and B. Scrosati, *Electrochim. Acta, 32* (1987) 961.
14 M. M. Thackeray, L. A. De Picciotto, A. De Kock, P. J. Johnson, V. A. Nicholas and K. T. Adendorff, *J. Power Sources, 21* (1987) 1.
15 M. Yoshio, S. Inoue, M. Hyakutake, G. Piao and H. Nakamura, *J. Power Sources, 34* (1991) 147.
16 N. Kumagai, S. Tanifuji and K. Tanno, *J. Power Sources, 35* (1991) 313.
17 K. M. Abraham, D. M. Pasquariello and E. B. Willstaedt, *J. Electrochem. Soc., 137* (1990) 743.
18 R. Koksbang, I. I. Olsen, P. E. Tonder, N. Knudsen and D. Fauteux, *J. Appl. Electrochem., 21* (1991) 301.
19 F. Croce, F. Capuano, A. Selvaggi and B. Scrosati, *J. Power Sources, 32* (1990) 381.
20 W. J. Mackin, R. J. Neat and R. J. Powell, *J. Power Sources, 34* (1991) 39.